Integrating Materials and Manufacturing Innovation (2024) 13:175–184
https://doi.org/10.1007/s40192-023-00336-0

THEMATIC SECTION: ADDITIVE MANUFACTURING BENCHMARKS 2022

Ability to Simulate Absorption and Melt Pool Dynamics for Laser Melting of Bare Aluminum Plate: Results and Insights from the 2022 Asynchronous AM-Bench Challenge

Brian J. Simonds[1] · Jack Tanner[1] · Alexandra Artusio-Glimpse[1] · Niranjan Parab[2] · Cang Zhao[2,3] · Tao Sun[2,4] · Paul A. Williams[1]

Received: 25 October 2023 / Accepted: 17 December 2023 / Published online: 1 February 2024

Abstract
The 2022 Asynchronous AM-Bench challenge was designed to test the ability of simulations to accurately predict laser power absorption as well as various melt pool behaviors (width, depth, and solidification) during laser melting of solid metal during stationary and scanned laser illumination. In this challenge, participants were asked to predict a series of experimental outcomes. Experimental data were obtained from a series of experiments performed at the Advanced Photon Source at Argonne National Laboratories in 2019. These experiments combined integrating sphere radiometry with high-speed X-ray imaging, allowing for the simultaneous recording of absolute laser power absorption and two-dimensional, projected images of the melt pool. All challenge problems were based on experiments using bare aluminum solid metal. Participants were provided with pertinent experimental information like laser power, scan speed, laser spot size, and material composition. Additionally, participants were given absorptance and X-ray imaging data from stationary and scanned laser experiments on solid Ti–6Al–4V that could be used for testing their models before attempting challenge problems. In total, this challenge received 56 submissions from eight different research groups for eight individual challenge problems. The data for this challenge, and associated information, are available for download from the NIST Public Data Repository. This paper summarizes the results from the 2022 Asynchronous AM-Bench challenge as well as discusses the lessons learned to help inform future challenges.

Keywords Additive manufacturing · Laser powder bed fusion · Absorption · Simulation

Introduction

In most laser-based additive manufacturing (AM), the energy absorbed from a high-power laser drives all process phenomena from melting to solidification. Therefore, accurate quantification of the laser absorptance is critical to accurately predict melt pool behavior and final part performance. As a result, organizers of the 2022 NIST additive manufacturing benchmark (AM-Bench) challenge series included a standalone challenge designed to test the ability of simulations to accurately predict laser power absorption as well as various melt pool behaviors during laser melting of solid metal. This was the first implementation of an asynchronous format, which is intended to be released more rapidly than the regular 3-year AM-Bench cycle.

Experimental data for this Asynchronous AM-Bench (A-AMB) challenge were obtained from a series of experiments performed at the Advanced Photon Source at Argonne National Laboratories in 2019 [1]. These experiments combined integrating sphere radiometry [2, 3] with high-speed X-ray imaging [4, 5], allowing for the simultaneous recording of absolute laser power absorption and two-dimensional, projected images of the melt pool. A schematic of this is shown in Fig. 1. These data are unique in that quantities important as simulation inputs (laser power and absorptance) are measured along with behaviors that can be predicted (melt pool dynamics).

The A-AMB challenge consisted of two sets of data: training data and blind challenge data. Training data

✉ Brian J. Simonds
brian.simonds@nist.gov

1 National Institute of Standards and Technology (NIST), Boulder, CO 80305, USA

2 Argonne National Laboratory, Lemont, IL 60439, USA

3 Tsinghua University, Beijing, China

4 University of Virginia, Charlottesville, VA, USA

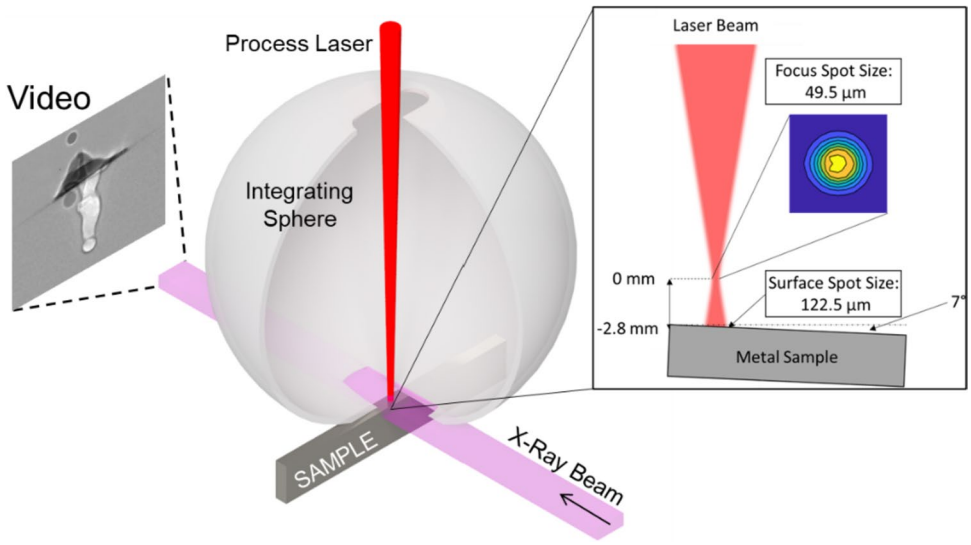

Fig. 1 Experimental setup with laser beam specifics given in the inset

Table 1 Challenge award structure

	Absorption	Geometry
Spot		
	Award#1 •Time-dependent absorption (TDA) •Average absorption (AA)	Award#2 •Time-dependent width (TDW) •Average solidification rate (ASR)
Scan		
	Award#3 •Time-dependent absorption (TDA) •Average absorption (AA)	Award#4 •Maximum depth and width •Average solidification rate (ASR)

included time-resolved absorptance and X-ray imaging data from stationary and scanned laser experiments on solid Ti–6Al–4V. These data were publicly released January 21, 2022, along with the modeling challenge problems that pertained to an Al alloy. Final challenge solutions were due April 22, 2022. Participants were provided pertinent experimental information like laser power, scan speed, laser spot size, and material composition for both sets of data. This format implicitly tested how well a model calibrated using data from one material (Ti–6Al–4V) could be applied to a different material (Al 5182) for which measurement results are not yet available. All data, training and blind, is currently available in the NIST Public Data Repository along with other useful experimental information [6].

The A-AMB blind challenge questions related to both stationary and scanned laser exposures on solid aluminum. Table 1 shows the award structure for the four challenge areas, with two problems per challenge area. Challenge problems included time-dependent absorption, average absorption before and after keyhole formation, melt pool dimensions, and solidification rates. Award winners were determined by the smallest normalized root-mean-square error (nRMSE) between the submitted answer and that determined experimentally. The average nRMSE for each award group was determined from the problems in that group. In total, the A-AMB challenge received 56 individual submissions from eight different research groups. Seven of the eight research groups were from academic institutions. Participants could choose how many and which of the eight problems to submit solutions for. Six participants submitted solutions to all eight problems, one submitted solutions to only the stationary spot problems, and one submitted only to the geometry problems.

Challenge Results

All blind challenge data was performed on solid Al 5182, which was cut from NIST standard reference material (SRM) 1241c [7]. To be compatible with the X-ray imaging technique, 1-mm-thick samples were cut from the SRM using wire electrical discharge machining. These were then polished to a mirror-like finish on all sides. X-ray images were captured at a rate of 50,000 frames per second with an exposure time of 2.5 µs for each frame.

The time resolution of the absorptance data was 40 ns for all measurements. The sample surfaces were tilted by 7° with respect to the horizontal plane in order for the integrating sphere to capture specularly reflected light from the initial surface. The laser diameter ($1/e^2$) at the sample surface was 122.5 µm, which was calculated from caustic measurements taken just before imaging and absorption experiments.

Stationary Spot Absorption

The first blind challenge was designed for a stationary laser beam on a bare aluminum plate. Figure 2 shows example data from these measurements. The bottom shows the relative absorption versus time for the entire 1.982 ms exposure. The absolute power absorbed is found by multiplying by the delivered power of 501 W. The top shows an example X-ray image obtained at the point in time marked by the red dot in the bottom plot. Participants were asked to predict the time-dependent absorption as well as the average absorption before and after keyhole formation. The presence of a keyhole was defined as the point in time, where the relative absorption was equal to or greater than 35%, which was approximately the steepest part of the absorption curve. From the graph in Fig. 2, this occurs at 0.189 ms (see also vertical dashed line in Fig. 3). Keyhole formation is strongly related to absorption [1, 8] due to multiple reflections of the processing laser within the keyhole cavity.

All submitted predictions for stationary laser time-dependent absorption are shown in Fig. 3 along with the NIST experimental value shown in red. Figure 4 shows the anonymized predictions for all participants who submitted predictions of absorption to the stationary laser spot category. The dashed horizontal lines in Fig. 4 show the experimental values. In general, participants underpredicted the average absorption before keyhole formation (Fig. 4a), whereas the predictions were more mixed when a keyhole was present (Fig. 4b). This observation most likely results from a reliance of the models on literature values for optical properties (Fresnel coefficients and dielectric constants, for instance) that are not representative of the aluminum material tested. Once a keyhole is formed, the dependence of the predicted absorption on these optical properties disappears as multiple reflection effects dominate.

The unique feature of the integrating sphere experiments is the ability to capture dynamic absorptance. These measurements reveal temporal fluctuations that are significantly larger than the measurement noise and are directly related to melt pool behavior [9]. Participants were asked to calculate the standard deviation of their predicted absorption during times when a keyhole was

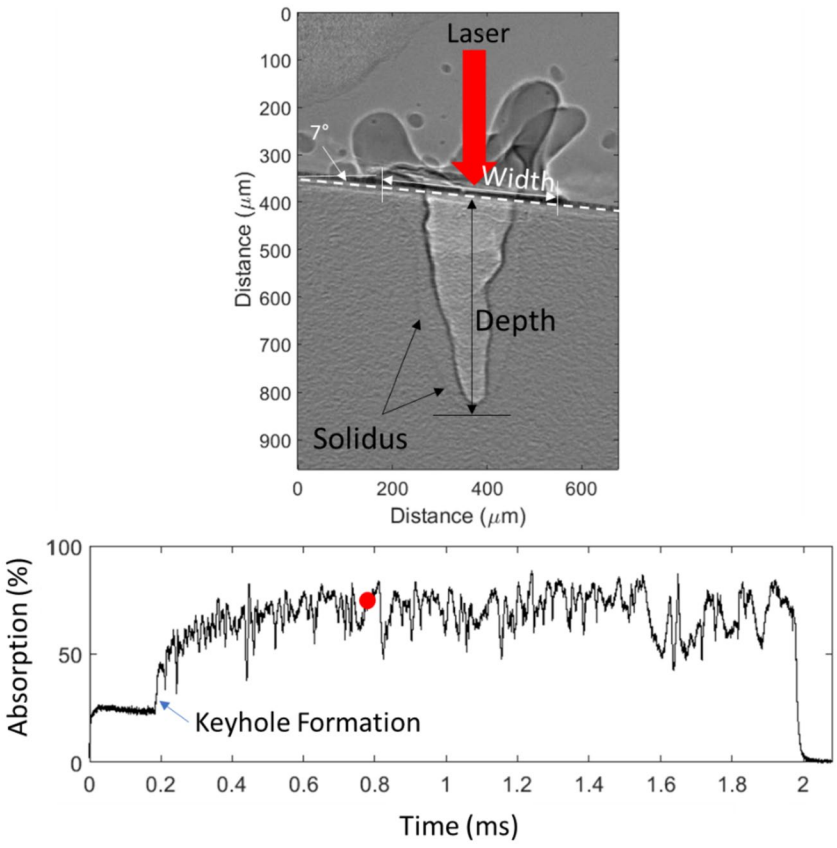

Fig. 2 An example stationary spot X-ray image with the corresponding absorption data. The top image corresponds to the melt pool at the point in time marked by the red dot in the plot below

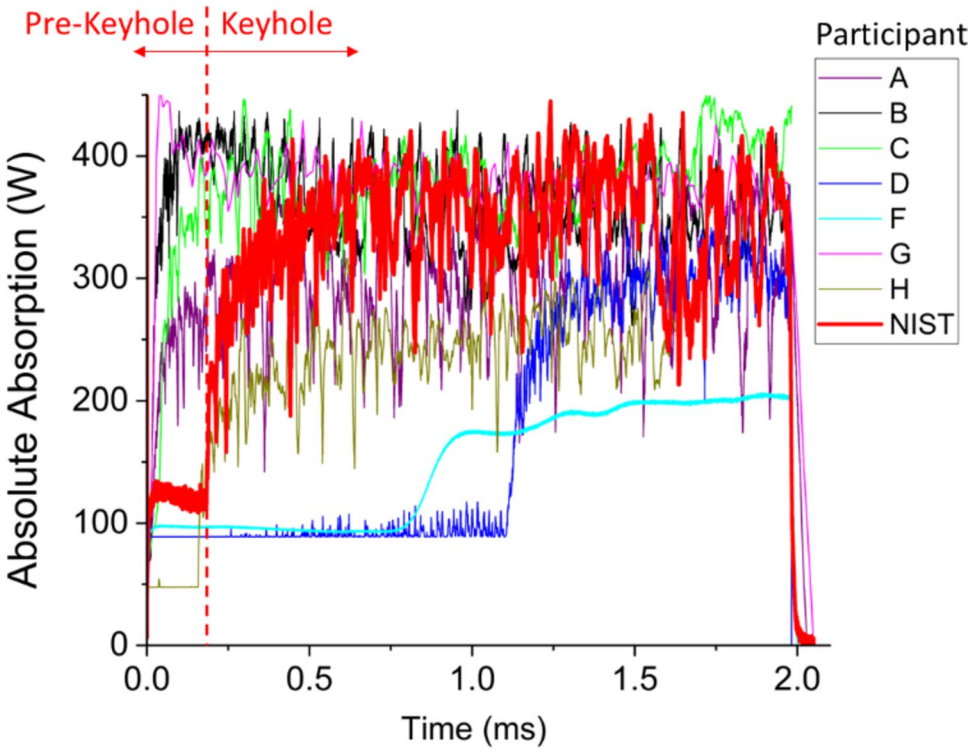

Fig. 3 Time-dependent absorption predictions from all participants along with the NIST experimental data

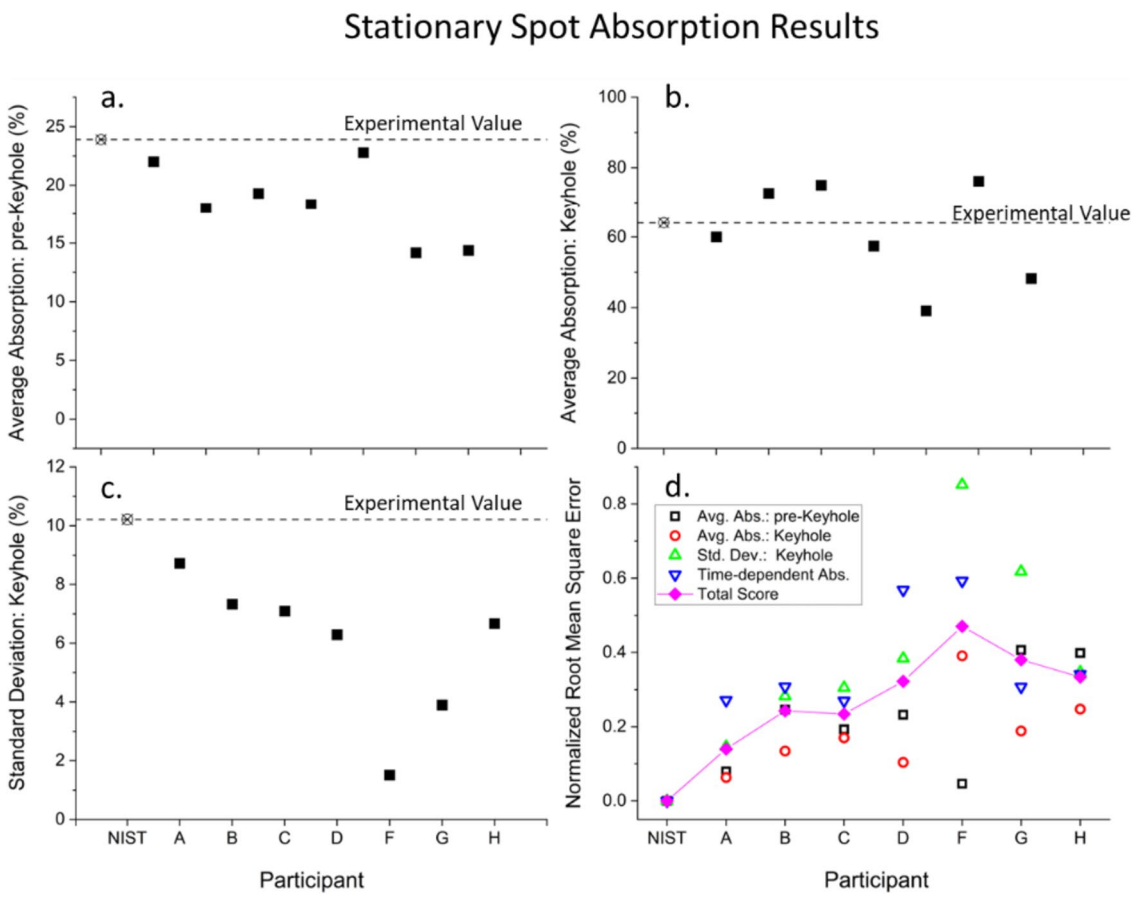

Fig. 4 Submitted predictions for average absorption before keyhole formation (**a**) and after (**b**) as well as the standard deviation of the time-dependent absorption when a keyhole is present (**c**). The total scores for the stationary spot absorption challenge are shown in (**d**)

present to determine if their simulations could accurately represent the dynamics measured during the experiment. These results, shown in Fig. 4c, illustrate that all simulations underpredicted the amount of absorption variability.

Figure 4d shows the individual scores for each participant calculated using the nRMSE method. The lower the value of nRMSE means a higher agreement with experiment. The nRMSE values for each problem were averaged to give the total score for this challenge, which is shown by the solid diamonds (and connecting line). The lowest average nRMSE was chosen as the challenge winner, which in this case was participant A. Tie second place awards were given to participants B and C.

Stationary Spot Geometry

The second challenge considered the melt pool geometry during a stationary laser exposure. Participants were asked to predict the time-dependent width of the melt pool and the average solidification rate. The width was defined as the lateral extent of the interface between liquid and solid along the initial metal surface (see Fig. 2 top). The solidification rate was measured as the rate of change of the melt pool depth as measured from the furthest extent of the solidus directly below the incoming laser beam (see Fig. 2 top).

The predicted time-dependent melt pool widths are shown in Fig. 5a, with roughly equal numbers of participants predicting higher and lower values than the experiment. Values for solidification rate (Fig. 5b) had significantly more variability with outliers from participants B, E, and F. It is believed that these outliers were due to either improperly following challenge instructions or incorrect units. However, in order to remain impartial and equitable to all participants A-AMB submissions were considered final. The nRMSE results (Fig. 5c) show that participant A again won first place, participant C won second, and participant H was given an honorable mention for their extremely accurate time-dependent melt pool width prediction.

Scanned Line Absorption

The third and fourth challenges were based on data from a scanned laser across a bare aluminum plate. For these challenges, the laser exposure was at 473 W for 1.980 ms moving at 700 mm/s. The image in Fig. 6 shows the scan direction across the metal surface.

As before, participants were asked to predict the time-dependent absorption as well as the average absorption before and after a keyhole cavity formed. For these measurements, the presence of a keyhole was defined as relative absorption greater or equal to 25% determined by where the change in absorption with respect to time was greatest. Figure 7 shows all submitted predictions for the

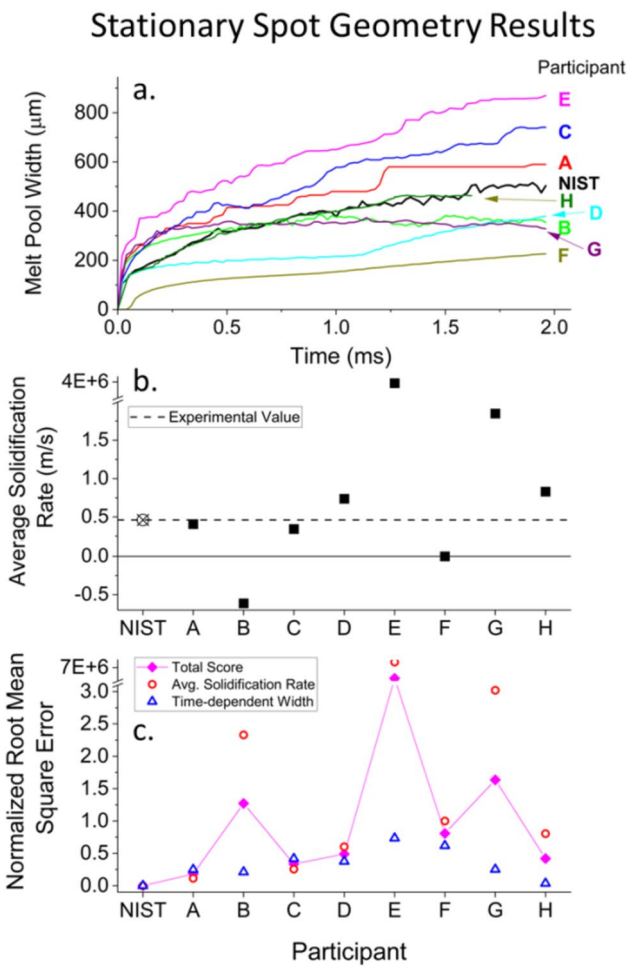

Fig. 5 Submitted predictions for melt pool width (**a**) and average solidification rate (**b**). The total scores for the stationary spot geometry challenge are shown in (**c**)

time-dependent absorption along with the experimental result in red. In comparison with the stationary results (Fig. 3), the spread in the predicted behavior is much larger, which suggests that the incremental increase in complexity of a scanned beam versus stationary, even over a very limited range, makes accurately predicting laser absorption more difficult. The chosen experimental time-dependent absorption data shows oscillatory behavior, the origins of which were discussed in a previous publication [9]. None of the simulations predicted these periodic oscillations.

The average absorption before and after keyhole formation are shown in Fig. 8. As with the stationary laser case, the submitted predictions universally underestimate the average absorption before keyhole formation but after keyhole formation their predictions agree much better on average with the experimental results. We believe that this is due to the same insufficient availability of accurate optical properties in the literature. Only one participant,

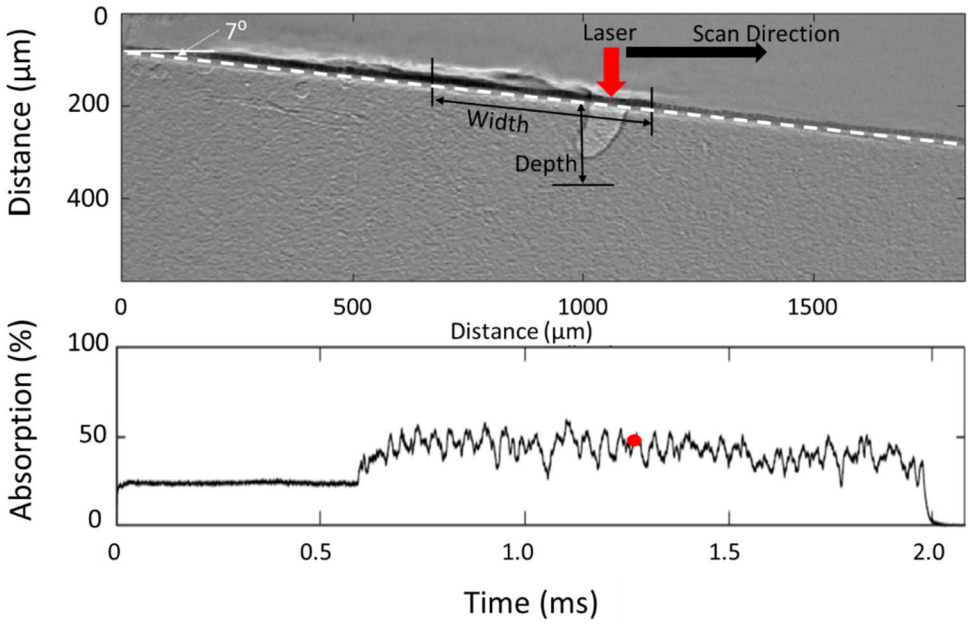

Fig. 6 An example X-ray image during the scanned laser experiments along with the corresponding absorption data. The top image corresponds to the melt pool at the point in time marked by the red dot in the plot below

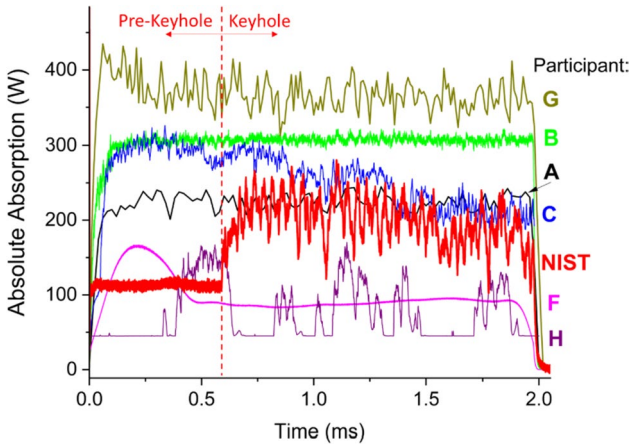

Fig. 7 Time-dependent absorption predictions from all participants including the NIST experimental data for the scanned laser on aluminum

participant C, predicted a standard deviation of the absorption that was similar to that measured experimentally with all others well below (Fig. 8c). The lowest nRMSE for first place was awarded to participant C with participant A in second (Fig. 8d).

Scanned Line Geometry

For the scanned laser, participants were asked to provide the maximum extent of the melt pool depth and width. The width is defined as the lateral distance along the original metal surface between the two solidus interfaces. The depth is defined as the deepest solidus interface measured relative to the original metal surface in a direction parallel to the incoming laser beam. These are shown in Fig. 6. These results are shown in Figs. 9a and b, respectively. With one exception, these quantities were universally overestimated. This could be due to a lack of appropriate thermophysical properties for this particular aluminum alloy or from differences in boundary conditions simulated versus actual. The submitted solidification rate predictions (Fig. 9c) have outliers similar to the stationary spot case, presumably for similar reasons. This challenge resulted in a tie for both first (participants F and H) and second place (participants A and B).

Discussion and Conclusion

Figure 10 shows a histogram of all awards given in the 2022 A-AMB with five of the eight participants winning at least one award. This broad distribution of awards suggests that no single simulation was dominant and that all models could be improved. Although participant identities are anonymized for publication, participants were informed of their own letter identifier and are allowed to reveal themselves to other participants if they choose. We believe that there is great value in disparate research groups comparing their unique methods, assumptions, and results when attempting to predict the same experimental conditions. The ability to do so is one great advantage of such benchmark tests.

There are other conclusions that can be drawn by comparing the simulation predictions to experimental results. The first is that the absorption before keyhole formation is universally underpredicted by simulation. This discrepancy disappears once a keyhole has formed. A potential cause

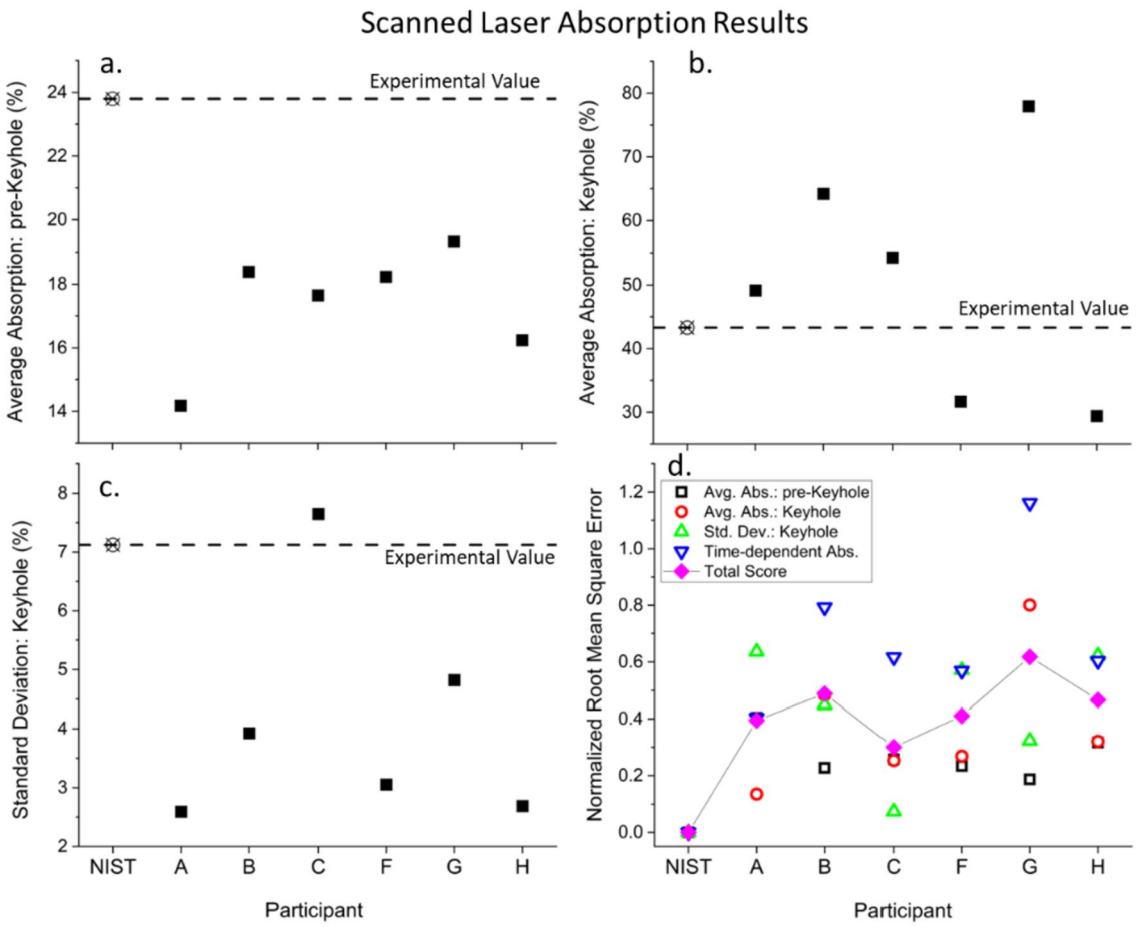

Fig. 8 Submitted predictions for average absorption before keyhole formation (**a**) and after (**b**) as well as the standard deviation of the time-dependent absorption when a keyhole is present (**c**). The total scores for the scanned line absorption challenge are shown in (**d**)

of this is that most simulations rely on literature values for optical properties and that these properties do not adequately describe the material used during the experiments. Since reflection and absorption are very sensitive to surface preparation, the experimental and literature values could deviate if the two surfaces are not identical. Once a keyhole forms, the absorption behavior is much less sensitive to optical properties as multiple reflections dominate. This is just one example of the larger issue of applying optical, thermal, and mechanical properties from literature to simulate specific experimental conditions.

Furthermore, most simulations overestimated melt pool width and depth for the scanned laser, whereas the predictions were more mixed for the stationary case. This could point to a boundary condition or thermophysical property discrepancy between experiment and simulation. At least one participant admitted that infinite boundary conditions were used for their simulations to increase computational efficiency. Since the samples had a high aspect ratio (1 mm by 26 mm), this could reasonably alter results. It was also pointed out by one participant that the laser beam caustic is rarely simulated, which creates a difference in the actual heat source and that simulated. The scanned laser measurements were repeated three times under identical conditions with the averages used for the final comparison to simulation. The average maximum melt pool depth and width with standard deviations were, respectively 88.8 μm ± 0.4 μm and 326 μm ± 16 μm, which shows good experimental repeatability.

This A-AMB challenge also sought to take advantage of the high time resolution of the absorptance data by asking modelers to quantify the dynamics of their predicted absorption. The metric chosen for this was the standard deviation of the absorption when a keyhole was present. In both the stationary and scanned laser cases, simulations nearly universally underpredicted the variability measured experimentally. Additionally, during the scanned laser case, the measured periodic oscillations [9] were not predicted by any group. This could possibly be explained by a lack of relevant liquid thermophysical properties, especially in liquid aluminum that could contain oxidation. Another possible explanation is that the vapor plume could be adding

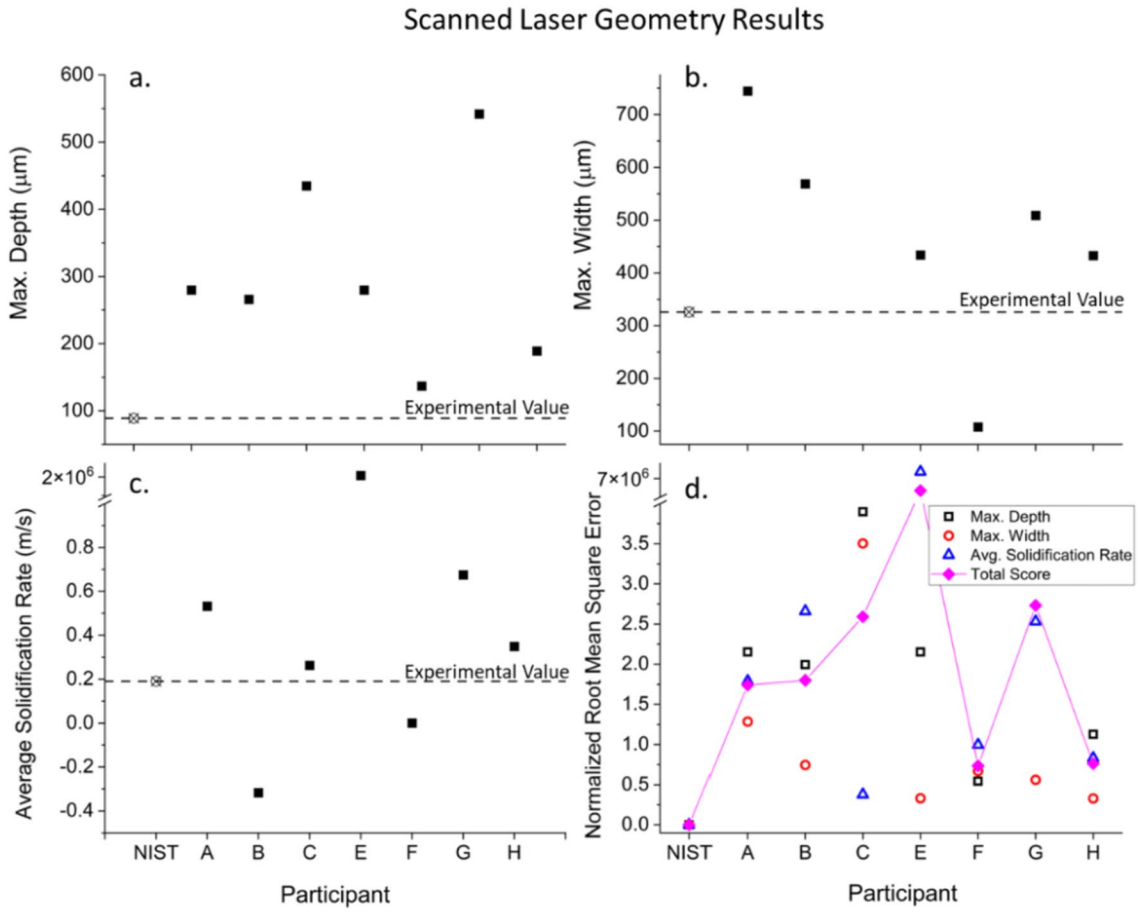

Fig. 9 Predictions for maximum melt pool depth (**a**), width (**b**), and solidification rate (**c**). The final scores for the scanned laser geometry problems are shown in (**d**)

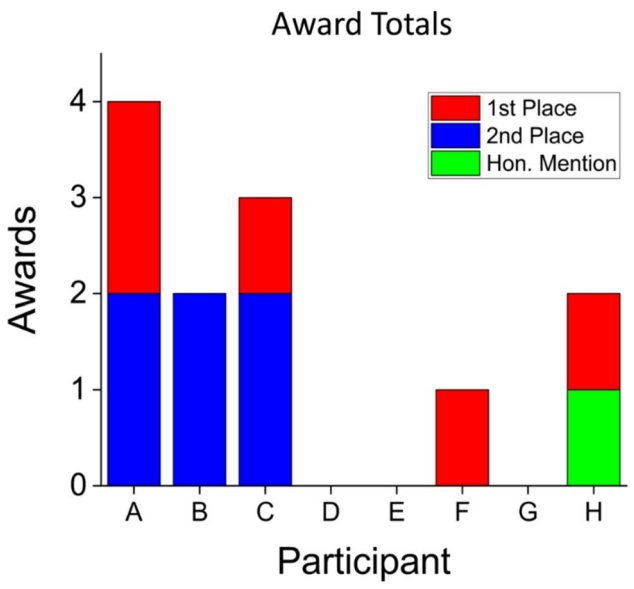

Fig. 10 Histogram of all awards given to participants in all A-AMB challenges

additional variability to the data that is not considered in most simulations.

Given the relatively large number of submissions to the 2022 A-AMB challenge, it is hoped that absorption will play a role in future AM-Bench challenges. From this inaugural absorption-based challenge, there are two specific recommendations. The first is to choose a material that is less variable than aluminum. Aluminum's variability is due to its high reflectivity and high thermal conductivity [10]. As a result, high initial laser powers must be used to melt the material and form a vapor cavity. Once formed, multiple reflections lead to significantly more laser energy absorption, which is seen in Fig. 3 as a nearly tripling of absorption within microseconds. Low initial absorption also means that the coupling is very sensitive to surface preparation as small imperfections can have a large relative increase in initial absorption in the solid. Figure 11 compares repeated measurements of solid Ti–6Al–4V and aluminum with a stationary laser exposure. The transition to form a keyhole is evidenced by the step increase in absorption, which for Ti–6Al–4V occurs very repeatably to within about 30 μs. In comparison, the aluminum data varies by 190

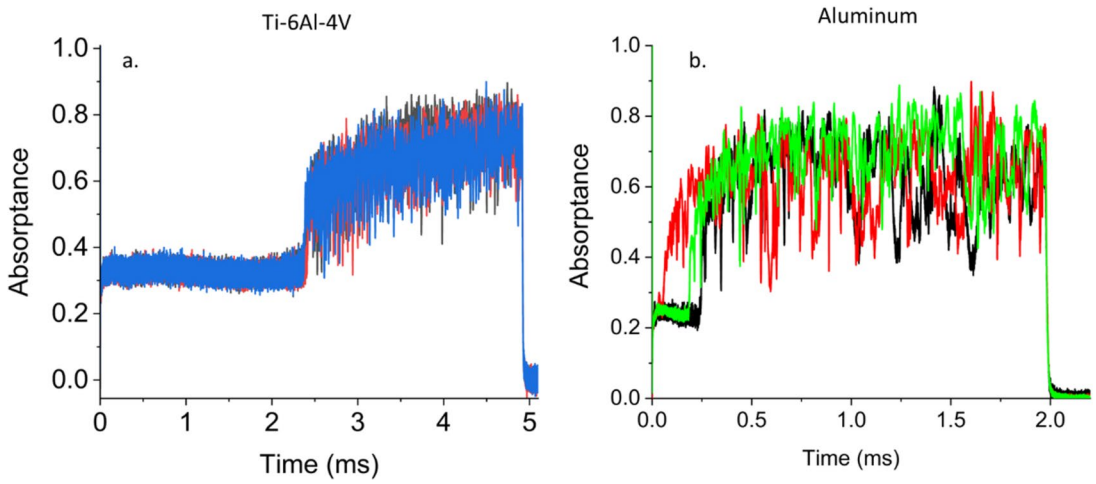

Fig. 11 Repeated absorptance measurements of solid **a** Ti–6Al–4V and **b** aluminum using a stationary laser exposure

μs for the stationary case and 650 μs for scanning. This led to different time dependencies of melt pool width and depth, which is why only the maximum values were used for the scanning case. Another instance of variability with aluminum was that there were occurrences where the melt pool would be completely or partially ejected. These events only occurred at relatively high laser powers but beyond that were random. Data were chosen well below this regime.

The second suggestion for future challenges is to acquire sufficient data to make statistically relevant statements, especially with respect to stochastic events like pore formation. The measurements discussed here were originally designed for separate studies on melt pool dynamics and not specifically for the A-AMB challenge. Although some repeated measurements were obtained, limitations of synchrotron beam time and other research objectives took precedent. Future experiments could be designed to prioritize repeated measurements for statistical analysis. As repeated measurements are obtained, it is also suggested that image analysis for obtaining melt pool dimensions be automated as much as possible.

Acknowledgements The authors thank all eight participants who submitted solutions to the 2022 A-AMB challenge problems. They also thank the organizers of the AM-Bench challenge series, Lyle Levine and Brandon Lane.

Declarations

Conflict of interest The authors do not have a conflict of interest pertaining to this work.

References

1. Simonds B, Tanner J, Artusio-Glimpse A, Williams PA, Parab N, Zhao C, Sun T (2021) The causal relationship between melt pool geometry and energy absorption measured in real time during laser-based manufacturing. Appl Mater Today 23:101049
2. Simonds BJ, Garboczi EJ, Palmer TA, Williams PA (2020) Dynamic laser absorptance measured in a geometrically characterized stainless-steel powder layer. Phys Rev Appl 13:024057
3. Simonds BJ, Sowards J, Hadler J, Pfeif E, Wilthan B, Tanner J, Williams P, Lehman J (2018) Time-resolved absorptance and melt pool dynamics during intense laser irradiation of metal. Phys Rev Appl 10:044061
4. Zhao C, Fezzaa K, Cunningham RW, Wen H, De Carlo F, Chen L, Rollett AD, Sun T (2017) Real-time monitoring of laser powder bed fusion process using high-speed X-ray imaging and diffraction. Sci Rep 7:3602
5. Parab ND, Escano LI, Fezzaa K, Everhart W, Rollett AD, Chen L, Sun T (2018) Ultrafast X-ray imaging of laser–metal additive manufacturing processes. J Synchrotron Radiat 25:1467
6. Simonds BJ, Tanner J, Artusio-Glimpse A, Williams PA, Parab N, Zhao C, Sun T, Asynchronous AM Bench (2022) Challenge data: real-time, simultaneous absorptance and high-speed xray imaging. National Institute of Standards and Technology, NIST Public Data Repository. (Accessed 10 Oct 2023). https://doi.org/10.18434/mds2-2525
7. Standard Reference Material 1241c, National Institute of Standards and Technology
8. Zhao C, Shi B, Chen S, Du D, Sun T, Simonds BJ, Fezzaa K, Rollett AD (2022) Laser melting modes in metal powder bed fusion additive manufacturing. Rev Mod Phys 94:045002
9. Khairallah SA, Sun T, Simonds BJ (2021) Onset of periodic oscillations as a precursor of a transition to pore-generating turbulence in laser melting. Addit Manuf Lett 1:100002

10. Zhang J, Song B, Wei Q, Bourell D, Shi Y (2019) A review of selective laser melting of aluminum alloys: processing, microstructure, property and developing trends. J Mater Sci Technol 35(2):270–284